Translational Oncology 14 (2021) 101211

Contents lists available at ScienceDirect

Translational Oncology

journal homepage: www.elsevier.com/locate/tranon

Original Research

A mechanistic insight into the anti-metastatic role of the prostate specific antigen

Francesco Pellegrino [a,b,1], Arianna Coghi [b,1], Giovanni Lavorgna [b], Walter Cazzaniga [a], Edoardo Guazzoni [c], Irene Locatelli [b], Isabella Villa [d], Simona Bolamperti [d], Nadia Finocchio [b], Massimo Alfano [b], Roberta Lucianò [e], Alberto Briganti [a,f], Francesco Montorsi [a,f], Andrea Salonia [a,f,1], Ilaria Cavarretta [b,1,*]

[a] Department of Urology, IRCCS San Raffaele Hospital, Milan, Italy
[b] Division of Experimental Oncology/Unit of Urology, IRCCS San Raffaele Hospital, Urological Research Institute, Via Olgettina, 60, Milan 20132, Italy
[c] Operative Unit of Orthopedics and Traumatology, Department of Clinical-Surgical Sciences, Diagnostics and Pediatrics, Fondazione IRCCS Policlinico San Matteo, Pavia, Italy
[d] Bone Metabolism Unit, Division of Genetics and Cell Biology, IRCCS San Raffaele Scientific Institute, Milan, Italy
[e] Pathology Unit, IRCCS San Raffaele Hospital, Milan, Italy
[f] Vita-Salute San Raffaele University, Milan, Italy

ARTICLE INFO

Keywords:
PSA
KLK3
Prostate cancer
Collagen I
Extracellular matrix
Metastasis

ABSTRACT

Aim: Since its discovery Prostate Specific Antigen (PSA), also referred to as kallikrein-3 (KLK3), has been used as standard circulating biomarker for prostate cancer (PCa). However, its specificity remains not adequate and its mechanism of action still elusive. Therefore, deciphering PSA role throughout PCa-pathobiology would be relevant in improving both cancer diagnosis and outcome prediction. We investigated the possible role played by PSA on/in the tumor microenvironment and over the first steps of cancer invasion.

Methods: Fresh PCa-specimens and cell lines were used for *ex-vivo/in-vitro* invasion assays and assessment of prostate tissue-PSA (tPSA), type 1 collagen (COL1A1) and ß1-integrin expression. Tissue Cancer Genome Atlas (TCGA) and Decipher® datasets were considered to estimate tPSA clinical relevance.

Results: A more precise, inverse, correspondence between tPSA and clinical/pathological parameters was found than for circulating PSA. *KLK3* combined with Gleason grade and pathologic stage, better predicted cancer-related mortality. Consistently, we demonstrated that PSA inhibits prostate extracellular-matrix (ECM) invasion by PCa cells. As for the mechanism of action, we provided novel information that PSA is able to cleave COL1A1, a main component of the ECM. Finally, ß1-integrin, a crucial COL1A1 transducing-receptor involved in tumor adhesion/invasion, resulted to be downregulated in PCa specimens with higher levels of tPSA.

Conclusions: By interfering with type 1 collagen and its downstream targets, PSA may hamper adhesion and path of the cancer cells through ECM and their migration ability, thus explaining the inverse correlation highlighted between prostate tPSA levels and clinically significant disease.

Introduction

Despite advances in cancer prevention, diagnosis and treatment, prostate cancer (PCa) remains one of the leading causes of male cancer death in Western countries [1,2]. Since its discovery in the '80, the prostate specific antigen (PSA) has been considered the marker for excellence for PCa [3,4], and therefore used as a paradigm of reference basically in all studies on novel biomarkers. Nevertheless, despite the high accuracy of nomograms including PSA in predicting clinical outcomes, the percentage of misdiagnosis remains significant [5–7], with heavy consequences in terms of morbidity, mortality and social costs. Surprisingly, in the face of thousands of publications on PSA as a biomarker, only few studies addressed its role in terms of PCa pathobiology [8–13]. Conversely, deciphering the biological role of PSA

* Corresponding author.
E-mail address: cavarretta.ilaria@hsr.it (I. Cavarretta).
[1] These authors contributed equally to this work.

https://doi.org/10.1016/j.tranon.2021.101211
Received 1 June 2021; Received in revised form 14 July 2021; Accepted 21 August 2021

throughout cancer progression may help to more comprehensively understand its clinical significance and limitations with a benefit in terms of cancer diagnosis and outcome prediction. PSA, also referred to as kallikrein-3 (KLK3), belongs to the family of glandular kallikrein-related peptidases with serine protease activity [14]. It is secreted from the apical end of luminal epithelial cells, stored at high concentrations in the prostatic collecting ducts and normally released into the seminal fluid. Its main physiologic role consists in maintaining semen fluidity by cutting semenogelin I and II. In the case of PCa, the alteration of the histological structure of the prostate causes a remarkable spillover of PSA into the surrounding stroma [15,16], where its levels may exceed of several orders of magnitude the levels of circulating PSA (cPSA). In this context, PSA has been reported to be active [16]. PSA may cleave also additional and different target molecules such as IGFBP-3, PTH-related protein, latent TGF-beta 2 and extracellular matrix (ECM) components (*i.e.*, fibronectin, collagen IV and XXIII, laminin and galectin-3) [8,13,16–18]. Overall, these observations prompted us to investigate the possible consequences of high prostate tissue-associated PSA (tPSA) levels toward type 1 collagen (COL1A1), one of the most abundant components of the prostate ECM, and toward PCa invasion. We hypothesize that, by altering the tumor microenvironment structure/composition, PSA activity on tumor ECM substrates has an impact on the PCa cell ability to enter the metastatic process. Of relevance, we also compared the net benefit of including tPSA rather than cPSA in the prediction of clinically significant PCa.

Materials and methods

Datasets

In case of the Tissue Cancer Genome Atlas (TCGA) dataset [19], normalized expression data and clinical data were taken from the Genomic Data Commons Data Portal (https://portal.gdc.cancer.gov/), whereas, in the case of the Decipher® dataset [20], access to data was obtained directly from Decipher Biosciences (Veracyte, San Diego, CA).

Statistical analysis

The Pearson correlation coefficient between *KLK3* mRNA expression and several clinical parameters was calculated both considering TCGA and Decipher® dataset by using the R software (https://www.r-project.org). Selected clinical variables were: primary and secondary Gleason score (then transformed into Gleason Grading Groups, GGG); pathological T-stage (pT); and, preoperative cPSA. Descriptive statistics, univariable (UVA) and multivariable (MVA) logistic regression analyses were performed to evaluate the association between *KLK3* expression and specific outcomes. Covariates for the multivariable models were identified with a stepwise forward selection approach and consisted of cPSA, pT, GGG and prostate tissue-*KLK3*. ROC curves and AUC calculation were used to quantify the discrimination ability of the different models. Decision Curve Analysis was calculated from the multivariable models to evaluate the net benefit of using *KLK3* expression to predict a specific outcome. *In vitro* experiments were repeated at least three times. *KLK3* mRNA expression was expressed as RPKMs (Reads Per Kilo Million). GraphPad Prism 8 (La Jolla, CA, USA) was used to create graphical representation and for statistical evaluation. The Mann-Whitney U test was applied to assess statistical significance. All tests were run using a significance level (p-value) set to 0.05.

Biobank specimens collection/processing

Prostate specimens were collected from patients undergoing radical prostatectomy (RP) for PCa at a single tertiary-referral academic institute. The protocol was approved by the Institutional Ethical Committee (Protocol URBBAN, 01.09.2010). All patients signed an informed consent agreeing to deliver their own anonymous information for future studies. Specimens were either vital frozen in the absence of serum to obtain ECM or immediately snap frozen in liquid nitrogen to obtain protein lysates. Seminal fluid was collected from healthy voluntary men, processed immediately by centrifugation at 5000 rpm and stored at −80 °C.

Reagents and prostate cell lines

All reagents and chemicals were from Thermo-Fisher Scientific Inc. (Waltham, Massachusetts, USA), unless otherwise stated. The human epithelial prostate cell lines RWPE-1 and RWPE-2 (RRID:CVCL_3791 and CVCL_3792) and the human metastatic MDaPCa2b (RRID:CVCL_4748) and PC3 (RRID:CVCL_4748) cell lines were purchased from ATCC and maintained as previously described [21,22]. RWPE-2 were maintained as RWPE-1. All cell lines were regularly tested for mycoplasma presence by amplifying a specific mycoplasma sequence; the primers utilized in the Polymerase Chain Reaction were ACTCCTACGGGAGGCAGCAGCAGTA (Forward) and TGCACCATCTGTCACTCTGTTAACCT (Reverse). PSA was from ExBio (Vestec, Czech Republic) and Merck Life Science. PSA antibody was from Santa Cruz (Heidelberg, Germany). Rabbit anti-integrin β1 was from Abcam (Milan, Italy). Secondary antibodies were from Biorad (Hercules, California, USA) and Cell Signaling Technologies (Danvers, MA, USA).

Western blot

Human prostate tissues were lysed by sonication (50% power; 15 pulses/cycles punctuated by a 1 s pause for a total of 1 min and 15 s). Cell lysate was obtained as previously described [23]. Equal amounts of proteins were resolved by SDS-PAGE and transferred onto PVDF membranes. After blocking, membranes were incubated overnight at 4 °C with the primary antibodies, followed by 1 h incubation with secondary antibodies. Signals were detected using the ECL method, according to the manufacturer protocol.

Tissue decellularization

Prostate tissue ECMs were obtained from RP specimens, previously marked by the pathologist as either tumoral or non-tumoral. Specimens were decellularized by using a protocol previously described [21,24] and then utilized in co-culture experiments.

EX vivo-in vitro 3D model of prostate stroma invasion

Prostate stroma invasion by prostate cells was evaluated in direct co-culture experiments, as previously described [21] by using non-tumoral prostate tissue-derived ECM, as a model of prostate tumor microenvironment, and the above described cell lines.

PSA activity

PSA activity on COL1A1 substrate was assessed by incubating either PSA or seminal fluid with the different substrates in PBS, for 22 h at 37 °C. The substrates were: human placenta-derived COL1A1 (Rockland Tebu-bio, Limerick, PA, USA), prostate ECM lysates and osteoblast cell lysates.

Primary osteoblast cultures

Description is reported in Supplementary Material and Methods.

Invasion assays with boyden chambers

Description is reported in Supplementary Material and Methods.

PSA elisa

Description is reported in Supplementary Material and Methods.

Guilt by association approach

Description is reported in Supplementary Material and Methods.

Results

PSA cleaves COL1A1

As type 1 collagen is one of the most abundant ECM components, we tested the action of PSA on this substrate. In order to recapitulate the extremely high PSA levels accumulating in the tumor microenvironment [8,16] during the first steps of invasion, we incubated the substrate, human COL1A1, with human seminal fluid (SF), which contains large amounts of PSA. We observed that SF completely degraded the substrate (Fig. 1A). This action was abrogated by an anti-PSA antibody, thus demonstrating that the effect is due to the PSA present in the human SF and not to other enzymes. PSA activity on COL1A1 was also verified on more complex substrates. In particular, a pool of SF from 6 different healthy subjects was able to cut the COL1A1 present in the ECM derived from human peripheral prostate tissue (Fig. 1**B**) and from human osteoblast primary cell cultures (**Suppl.** Fig. 1A). We finally tested the commercially available PSA considered in our next *in-vitro* assays, demonstrating it does cleave COL1A1 (**Suppl.** Fig. 1B). To verify whether COL1A1 is a substrate of PSA also *in-vivo*, we analyzed endogenous COL1A1 expression and degradation in 25 PCa resections from our institutional biobank in relation to their prostate tPSA content. Descriptive characteristics of patients are reported in Table 1; preoperative cPSA levels were found to be positively correlated with features of disease progression (*e.g.*, stage and lymph nodes invasion (LNI)), as expected by the known gate of this biomarker. By western blot analysis we observed downwards fluctuation of COL1A1 (185, 175 and 135 kDa), paralleled by a significant increase of its cleaved forms (63 and 40 kDa) in samples with higher tPSA expression (Fig. 2A,B). Samples were assigned to low-tPSA and high-tPSA groups according to an arbitrary PSA cutoff (corresponding to an optical density value of 30,000), which allowed us to discriminate patients with LNI and pathological stages higher than pT3a (Fig. 2**C**). Moreover, a significant correlation was observed between tPSA and 40 kDa COL1A1 ($r = 0.761$; $p < 0.0001$).

Table 1
Descriptive characteristics of patients from the IRCCS OSR institutional biobank.

	Age at surgery years (median + ES)	n. specimens/ patients	Preop. cPSA levels ng/ml (mean ± ES)
PCa patients	62 ± 1.42	25	12.83 ± 3.05

Pathological features	n. specimens/ patients	Preop. cPSA levels ng/ml (mean ± ES)	Statistical Significance of preop. cPSA levels
GS < 4+3	5	7.39 ± 1.60	
GS 4+3	9	12.67 ± 3.60	
GS 8	1	2	
GS 9	11	16.41 ± 6.51	
< pT3a	6	4.39 ± 0.97	
pT3a	7	11.66 ± 4.11	
> pT3a	13	17.36 ± 5.44	** *vs* <pT3a; * *vs* ≤ pT3a
pN0	18	8.16 ± 1.79	
pN1	8	23.33 ± 8.24	* *vs* N0

Abbreviations: cPSA: circulating serum PSA; pN0: without lymph node invasion; pN1; with Lymph node invasion

Fig. 2**D** details tPSA expression, normalized to the levels of actin, from the same samples plotted against pathological features. Significant differences were observed for higher grades and stages of the disease. These findings demonstrate that (i) PSA is able to cut COL1A1 *in vitro*; (ii) COL1A1 expression decreases in correspondence of higher tPSA; (iii) tPSA levels trend, measured in the PCa tumor microenvironment, parallels the extent of COL1A1 cleavage; and, (iv) both PCa tPSA content and corresponding COL1A1 cleavage inversely correlate with worse clinicopathological outcomes.

Tissue KLK3 gene expression inversely correlates to clinicopathological features and collagen expression

In order to confirm our findings on a wider case-study, we analyzed the well-established cohort of PCa patients of TCGA [19] and of the more

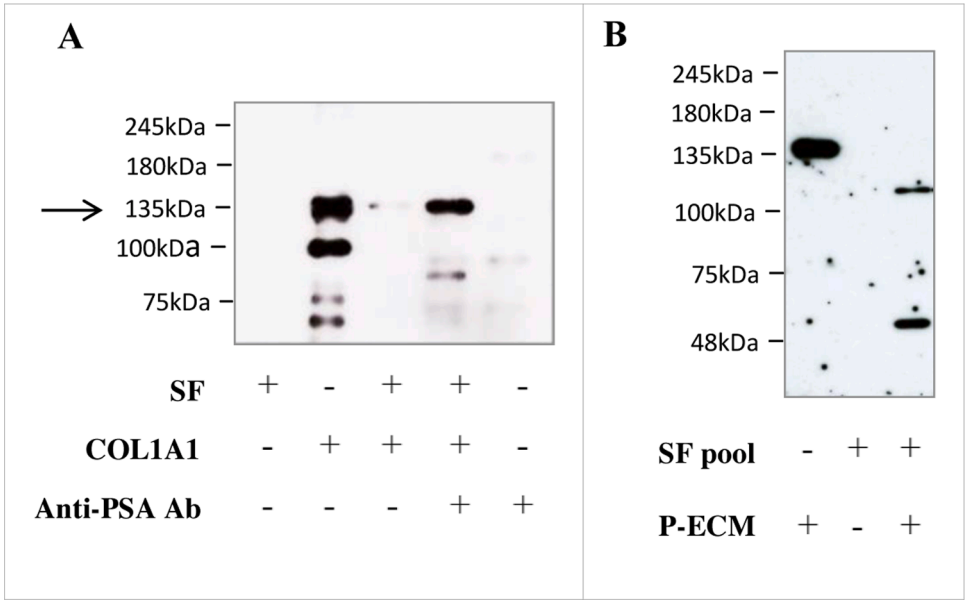

Fig. 1. Protease activity of PSA on COL1A1. COL1A1 cleavage by PSA was verified by western blot analysis on diverse substrates after incubation with or without Seminal Fluid (SF) for 22 h at 37 °C. Representative blots showing COL1A1 expression. (**A**) Human COL1A1 (3μg; 100μg/ml) was incubated with seminal fluid (SF) (53 μg; 1,77 mg/ml containing at least 50 μg/ml PSA), anti-PSA antibody (1 μg; 33 μg/ml) or both. Equal amounts of final product were loaded. The arrow indicates the band corresponding to COLL 1A1. Band disappears after incubation with SF1 but not when co-incubated with the anti-PSA antibody. The band at 100 KDa corresponds to COL1A2. Lower bands are most probably products of degradation. (**B**) ECM from prostate tissue (12 μg; 400 μg/ml) was lysed and incubated with or without a pool of SF from 6 different donors.

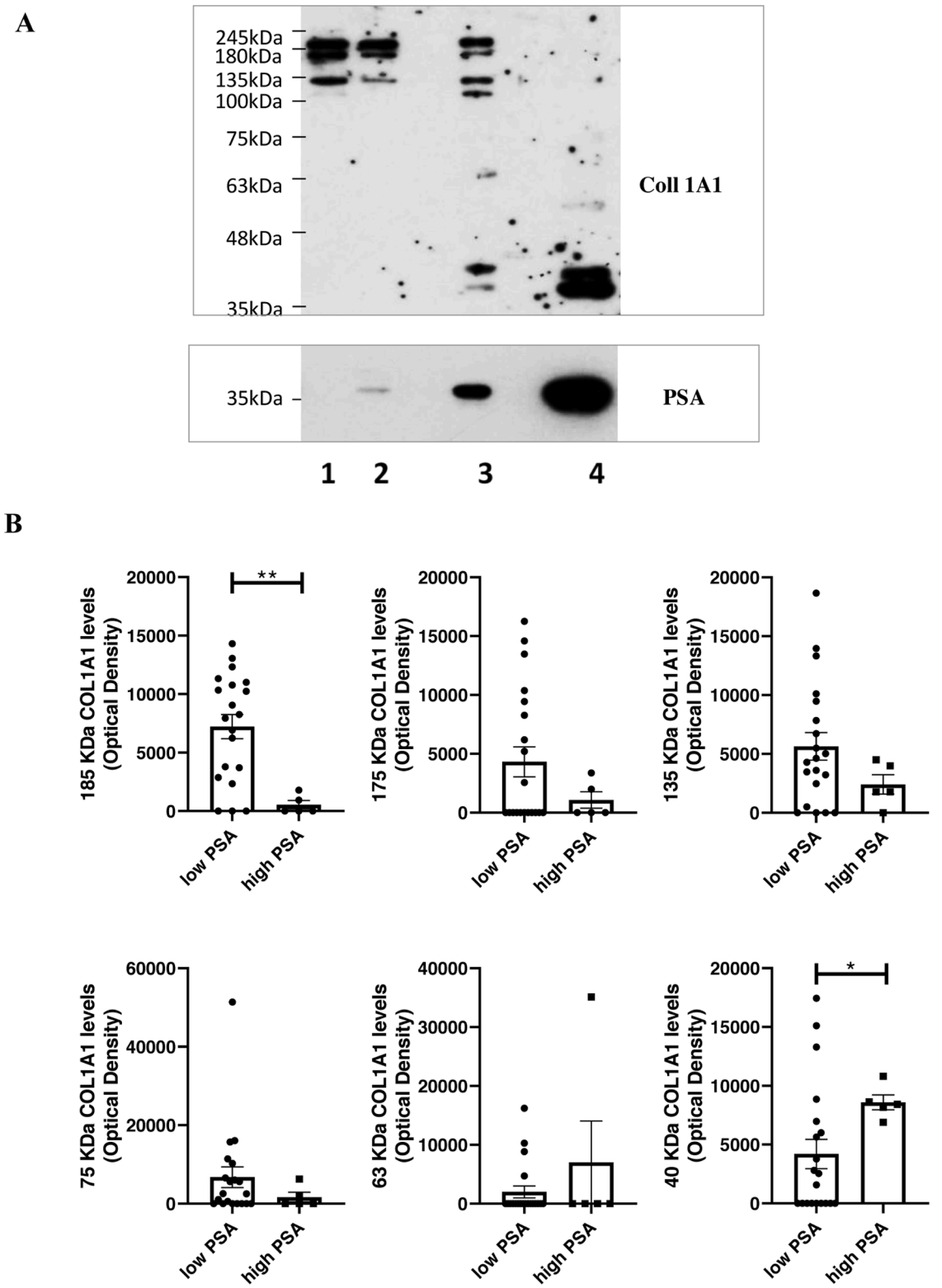

Fig. 2. Protein expression levels of tPSA and COL1A1 in human PCa specimens. PSA and COL1A1 levels were quantified by western blot analysis in surgical resections from RP. Specimens are from our institutional biobank. Equal micrograms of tissue lysate were loaded. (**A**) Representative blot images showing COL1A1 expression from samples with different PSA levels. COL1A1 and PSA were quantified on the same blot. (**B**) Plots showing quantification of COL1A1 and cleavage products of COL1A1 according to PSA levels. (**C**) Table showing number of cases, pathological features and statistical differences among groups with low or high PSA expression. (**D**) Plots showing protein PSA levels, normalized to the level of actin, according to grade, stage and lymph node positivity (LN1). Mean values ± SEM are reported. *$p < 0.05$; **$p < 0.01$; ****$p < 0.0001$ Mann-Whitney test.

C

	low PSA < 30000 O.D.	high PSA > 30000 O.D.
n. patients (i.e. specimens)	20 (100%)	5 (100%)
n. patients with pN1	8 (40%)	0 (0%)
n. patients with PCa stage ≥ pT3b	14 (70%)	0 (0%)
n. patients with PCa GS ≥9	10 (50%)	1 (20%)
Preop. cPSA (ng/ml; mean ± SEM)	13.39 ± 4.15	12.33 ± 6.07
tPSA (O.D.; mean ± SEM)****	11753.95 ± 2849.48	49496.8 ± 8149.36

D

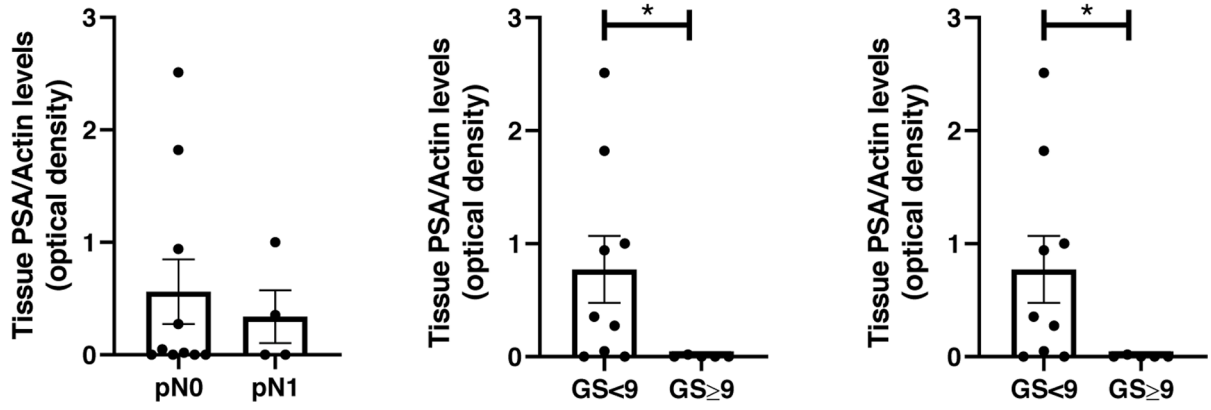

Fig. 2. (*continued*).

recent Decipher® dataset [20], which considers several more metastatic cases. In order to be used for calculation of the correlation coefficient, categorical variables 'pathologic T' and 'clinical T' were converted to numerical variables by using a progressive numbering. In TCGA, we observed a significant inverse correlation between *KLK3* gene expression and the number of positive LNs, c-stage (cT), p-stage (pT), and Gleason score (GS) (Table 2). In the Decipher®, in addition to LNI, stages and GS, a significant correlation between *KLK3* and preoperative cPSA, biochemical recurrence (BCR), metastases (MET), time to MET, PCa-related specific mortality (PCSM) and time to PCSM was also observed (**Table 3**). Thereof, we focused on the Decipher® dataset and further investigated the correlation and predictive value of *KLK3* expression on PCa progression/adverse outcomes. Descriptive characteristics of the entire cohort are summarized in **Suppl.** Table 1. Prostate tissue-*KLK3* expression levels were significantly lower among patients with LNI, BCR, MET and for those who died from PCa (**Table 4A,b**). At UVA logistic regression analysis, *KLK3* expression emerged to be associated with BCR, MET and PCSM, while no significant association was observed with nodal status (**Table 5**). The discriminative ability of each individual UVA model was graphically displayed with ROC curves (**Fig. 3A**); the calculated AUC were comparable for Gleason Grade Group (GGG), pT and *KLK3* expression and were higher than the AUC obtained for preoperative cPSA for each of the analyzed outcome. At MVA logistic regression analysis, *KLK3* expression emerged as a significant predictor of MET and PCSM (**Table 6**). Likewise, ROC curves and AUC were calculated for both MVA models (*i.e.*, with and without *KLK3*); hence, adding *KLK3* expression as a covariate improved the model performance in terms of MET and PCSM prediction, while no effect was observed on BCR (**Suppl.** Fig. 2). Decision-curve-analysis showed the net benefit of including *KLK3* expression to predict PCSM in comparison to not including *KLK3* gene expression (**Fig. 3B**). Finally, we highlighted an inverse correlation between *KLK3* mRNA and several collagens including COL1A1 (**Suppl.** Table 2).

PSA inhibits PCa invasion in vitro

We questioned whether PSA action on different stromal substrates, including COL1A1, may affect PCa cell escape from the primary tumor site toward the future metastatic niche. In this context, as an index of local invasion, we considered PCa cell movement through the ECM

Table 2
Correlation of prostate *KLK3* mRNA expression and preoperative circulating serum PSA levels to clinical parameters in patients with primary prostate tumors from the TCGA dataset ($n = 497$).

	r		p		n	
	KLK3	Preop. cPSA	*KLK3*	Preop. cPSA	*KLK3*	Preop. cPSA
KLK3	1	0.0119	0	1	497	482
Preop. cPSA value	0.0119	1	0.79	0	482	482
days to birth	0.1107	0.0174	0.01	0.71	486	471
age at initial pathologic diagnosis	−0.1189	−0.0294	0.01	0.52	497	482
number of LNs positive by H&E	−0.1594	0.2250	0.00	6.47E-06	406	394
numeric pathologic T	−0.3013	0.3087	9.7E-12	5.97E-12	490	475
numeric clinical T	−0.1606	0.2034	0.00	4.45E-05	405	397
Gleason pattern secondary	−0.2389	0.0788	7E-08	0.084	497	482
Gleason pattern primary	−0.2664	0.2605	1.6E-09	6.44E-09	497	482
Gleason score	−0.3403	0.2230	6.2E-15	7.62E-07	497	482

Abbreviations: cPSA: circulating serum PSA; LN: lymph nodes; H&E: hematoxylin and eosin; numeric pathologic T: numeric pathologic T stage; numeric clinical T: numeric clinical T stage.

itself. A previously developed 3D *ex-vivo/in-vitro* model consisting of decellularized prostate tissue samples [21] was implemented as a model of tumor microenvironment and prostate cell lines. In particular, we utilized RWPE-1 and RWPE-2 cell lines as a model of non-tumoral and tumoral, non-metastatic prostate cells, respectively. We also included the two metastatic PC3 and MDaPC2b prostate cell lines [25]. Before testing PSA involvement on PCa cell invasion, we ruled out possible misinterpretations due to the endogenous PSA production by performing PSA ELISAs on the prostate cell lysates and conditioned media. In our working conditions, the endogenous amount of PSA resulted to be basically null for all cell lines but MDaPCa2b (**Suppl. Table 3**). The different cell lines were thus put in direct co-culture with non-tumoral, peripheral prostate-derived ECM, as previously reported [21] (**Fig. 4**). Histological examination of the FFPE-ECM from the different co-cultures confirmed previous findings, thus showing a different pattern and extent of ECM invasion, consistent with and dependent on the known invasive ability of the different cell lines [21] (**Fig. 4A**). Although tumoral, RWPE-2 cells are non-metastatic and, consistently with their phenotype, significantly differ from PC3 in terms of invasive ability (**Fig. 4A,B**). When comparing basal invasive ability of PC3 (PSA-) and MDaPCa2b cells (PSA+), we observed that MDaPCa2b did not show any sign of invasion as compared with PC3 cells (**Fig. 4C**). Subsequently, the invasive ability of a single cell line with and without PSA treatment was tested. Any consistent effect of PSA on ECM invasive ability by the non-tumoral cells (RWPE-1) was observed, whereas a decrease of ECM invasion was depicted for tumoral cell lines. This was more pronounced for RWPE-2 compared to PC3 cells (**Fig. 4D**). The effect of PSA on invasion ability was also confirmed by using a different model of invasion. In depth, since most PCa metastases are bony, an *in vitro* surrogate of bone was recapitulated by using primary cultures of human osteoblasts.

Table 3
Correlation of prostate *KLK3* mRNA expression to clinical parameters in tumors from Decipher® ($n = 6577$).

	r		*p*		*n*	
	KLK3	Preop cPSA	*KLK3*	Preop cPSA	*KLK3*	Preop cPSA
pathgs p	−0.1409	0.1211	6.12E-26	7.77E-12	6076	3861
pathgs s	−0.0918	0.0467	1.32E-10	2.58E-01	6076	3861
preop cpsa	−0.0470	1.0000	2.51E-02	0.00E+00	5994	5994
age	−0.0061	0.0005	1.00E + 00	9.76E-01	6577	4347
svi	−0.1784	0.2177	2.71E-44	1.13E-46	6365	4242
epe	−0.0747	0.1269	3.32E-07	1.02E-16	6384	4252
sm	0.0102	0.0772	1.00E + 00	3.84 E-07	6487	4310
lni	−0.1063	0.1928	5.65E-14	1.32E-34	5883	3975
clings p	−0.1627	0.2017	4.40E-11	3.72E-16	2000	1600
clings s	−0.1084	0.1426	1.40E-04	1.00E-08	2000	1600
bcr	−0.1980	0.1278	1.45E-13	9.06E-07	1626	1468
bcr time	0.0312	−0.1098	1.00E + 00	3.33E-05	1578	1422
met	−0.1671	0.1206	2.00E-09	3.6E-06	1626	1468
met time	−0.1563	−0.0213	3.32E-07	4.21E-01	1447	1422
pcsm	−0.2029	0.1164	1.23E-12	2.62E-05	1447	1298
pcsm time	−0.2321	0.0427	3.05E-15	1.24E-01	1315	1297
capra s	−0.0690	0.5035	1.00E + 00	2.40E-69	1062	1062
adt	−0.2317	0.1935	1.55E-14	6.53E-12	1261	1239
rt	−0.0255	0.0588	1.00E + 00	2.66E-02	1446	1421
adt a	−0.0172	0.2103	1.00E + 00	4.27E-09	780	765
adt s	−0.1563	0.1283	1.60E-05	1.71E-05	1131	1116
rt a	0.0736	0.0094	1.00E + 00	7.80E-01	910	888
rt s	0.0053	0.0340	1.00E+00	1.20E-01	1446	1421
KLK3	1.0000	−0.0470	0.00E+00	2.73E-04	8626	5994
TotalPathGS	−0.1702	0.1186	1.05E-40	1.44E-13	6076	3861
TotalClinGS	−0.1768	0.2256	1.63E-15	6.64 E-20	2000	1600
Numeric pstage	−0.1811	0.1692	1.14E-45	1.13E-26	6034	3939
Numeric cstage	−0.0614	0.1793	2.82E-02	1.04E-09	1277	1143

Abbreviations: bbpathgs_p: primary pathological Gleason score; pathgs_s: secondary pathological Gleason score; preop_psa: preoperative psa;; svi: seminal vesicle invasion; epe: extra prostatic extension: sm: urgical margins; lni: lymph node invasion: clings_p: primary clinical Gleason score; clings_s: secondary clinical Gleason score; bcr: biochemical recurrence (0=no; 1=yes); bcr_time: time from RP to biochemical recurrence; met: metastasis (0=no; 1=yes); met_time: time from RP to metastasis; pcsm: prostate cancer specific mortality (0=no; 1=yes); pcsm_time: time from RP to pcsm; capra_s: CAPRA_S nomogram score; adt: androgen deprivation therapy received (0=no; 1=yes); rt: radiation therapy received (0=no; 1=yes); adt_a: adjuvant adt received (0=no; 1=yes); adt_s: salvage adt received (0=no; 1=yes); rt_a: adjuvant rt received (0=no; 1=yes); rt_s: salvage rt received (0=no; 1=yes). PathGS: pathological Gleason score; ClinGS: clinical Gleason score; pstage: pathological tumor stage; cstage: clinical tumor stage.

Table 4A
Descriptive statistics between patients' groups stratified according to the different outcomes (LNI, BCR).

	No LNI	LNI	*p*	No BCR	BCR	*p*
No. patients (%%)	489 (83.8)	94 (16.2)		236 (40.5)	347 (59.5)	
KLK3			0.05			<0.001
Median (IQR)	3.7 (3.2–4.1)	3.5 (3.0–4.0)		3.8 (3.4–4.2)	3.6 (3.0–4.0)	
GGG no.(%%)			< 0.001			< 0.001
= < 2	223 (45.6)	26 (27.7)		121 (51.3)	128 (36.9)	
3	95 (19.4)	12 (12.8)		45 (19.1)	62 (17.9)	
4	59 (12.1)	13 (13.8)		31 (13.1)	41 (11.8)	
5	112 (22.9)	43 (45.7)		39 (16.5)	116 (33.4)	
pT Stage			0.04			< 0.001
pT2	194 (39.7)	37 (39.4)		125 (53.0)	106 (30.5)	
pT3a	173 (35.4)	23 (24.5)		76 (32.2)	120 (34.6)	
pT3b	122 (24.9)	34 (36.2)		35 (14.8)	121 (34.9)	
Preop. cPSA (ng/ml)			< 0.001			1
Median (IQR)	8.5 (5.8–12.9)	11.9 (6.6–18.8)		8.9 (5.8–13.2)	8.7 (5.9–14.4)	
LNI no. (%%)	–	–	–			< 0.001
No	–	–	–	217 (91.9)	272 (78.4)	
Yes	–	–	–	19 (8.1)	75 (21.6)	
BCR no.(%%)			< 0.001	–	–	–
No	217 (44.4)	19 (20.2)		–	–	–
Yes	272 (55.6)	75 (79.8)		–	–	–
Time to BCR (months)			< 0.001	–	–	–
Median (IQR)	60.0 (24.0–96.0)	23.5 (12.0–57.3)		–	–	–
Metastasis no.(%%)			< 0.001			< 0.001
No	346 (70.8)	36 (38.3)		235 (99.6)	147 (42.4)	
Yes	143 (29.2)	58 (61.7)		1 (0.4)	200 (57.6)	
Time to MET (months)			< 0.001			< 0.001
Median (IQR)	82.0 (59.0–120.0)	60.0 (24.0–99.1)		93.6 (60.2–120.7)	65.4 (36.0–108.0)	
PCSM no.(%%)			< 0.001			< 0.001
No	427 (87.3)	67 (71.3)		236 (100.0)	258 (74.4)	
Yes	62 (12.7)	27 (28.7)		0 (0.0)	89 (25.6)	
Time to PCSM (months)			0.09			0.9
Median (IQR)	96.0 (61.3–130.6)	84.0 (58.1–121.4)		93.6 (60.2–120.7)	96.0 (60.0–132.0)	

Lymph Node Invasion (LNI) (at surgery) and Biochemical Recurrence (BCR) were coded as categorical variables with two levels (0 or 1). Data regarding time to the specific outcome were also obtained. **Abbreviations:** LNI (lymph node involvement at surgery); BCR (Biochemical recurrence); Statistical test: Kruskal-Wallis; significance level set: 0.05.

Here, PSA was found to inhibit the invasive ability of RWPE-2 cells toward the osteoblasts (**Suppl.** Fig. 3**A,B**) and toward the conditioned medium from osteoblasts (**Suppl.** Fig. 3**C**). Also in this model, PC3 depicted greater ability to invade than MDaPC2b cells (**Suppl.** Fig. 3**D, E**). In order to get insight into the mechanisms linking tPSA levels/activity, the altered COL1A1 expression/cleavage and the impaired PCa cell invasive ability, we looked at the ß1-integrin, which is the main collagen 1 transducing receptor regulating cancer cell adhesion, migration and invasion [26–28]. By western blot analyses we found decreased levels of ß1-integrin in correspondence of higher tPSA levels and COL1A1 cleavage or lower COL1A1 levels (**Fig. 5**).

Discussion

Current findings provide novel evidence that COL1A1 is an additional tissue-substrate for PSA. As for *in vivo* tPSA activity, we utilized human PCa specimens, demonstrating a correspondence between higher tPSA protein expression and low-to-null COL1A1 expression, paralleled by high COL1A1 cleavage; this envisages PSA *per se* is enzymatically active in the tumor milieu. Notably, PSA activity measured in prostate tissue has been previously reported to be inversely correlated to tumor aggressiveness and PCa cell invasive abilities [16,29–31]. In addition, our dataset analysis highlighted a consistent inverse correlation between *KLK3* and several types of collagens, including COL1A1. The inverse correlation among *KLK3* expression and such a broad range of collagens, together with additional PSA-substrates (as IGFBP-3, $r = -0.376$ $p =$ 3.35E-18; nidogen 1, $r = -0.335$ $p =$ 1.66E-14; laminin, $r = -0.345$ $p =$ 3.28E-15; fibronectin, 1 $r = -0.154$ $p =$ 7,7E-4;) suggests a more than a marginal action of PSA in the tumor microenvironment. By employing a 'guilt by association' approach [32], we indeed observed a consistent and consisting enrichment in pathways related to cell movement, invasion, matrix remodeling, and TGF-beta signaling among patients with low *KLK3* levels (Suppl. Table 4), which further supports the relevance of tPSA content on the structure and function of the ECM in dictating disease progression. Whether these correlations are causative, direct, or indirect deserves to be elucidated in future studies; however, our *in vitro* activity tests clearly suggest PSA does actively participate into this ECM-remodeling.

In parallel, we demonstrated that PSA hampers invasive abilities of PCa cells throughout both human prostate-derived ECM and Matrigel supports. This is true for both endogenous PSA (inferred by the comparison between the PSA- PC3 and the PSA+ MDaCa2b cells) and exogenous PSA levels (inferred by the comparison between vehicle- and PSA-treated cell lines), thus excluding possible misinterpretations due to the different PCa cell phenotype. This seemly counterintuitive observation, where PSA suppresses tumor cell migration even though it is cleaving ECM sustrates, becomes understandable if we consider the complexity of the ECM composition and the multiplicity of the signals arising from the tumor microenvironment. COL1A1, is, in fact, not only one of the main structural components of the ECM, but also an important mediator of ECM signaling. In particular, ß1-integrin is one of the main COL1A1 transducing receptors, which modulates invasive ability of cancer cells through activation of downstream signaling pathways such as those regulated by FAK, AKT and ERK [26–28]. PSA, by interfering with the integrity/activity/availability of COL1A1 integrin receptors, may obstacle the binding of PCa cells to ECM, thus inhibiting processes of cell adhesion and movement through the ECM itself. As a matter of fact, we showed a decreased expression of ß1-integrin in PSA+ versus PSA- specimens. Consistently, COL1A1 has been reported to be involved in cell adhesion and motility pathways of a number of tumors [26,27]. Additional effects as the well documented anti-angiogenic activity of PSA [33] also account for the minor cancer cell spread observed in the

Table 4B
Descriptive statistics between patients' groups stratified according to the different outcomes (MET, PCSM).

	No MET	MET	*p*	No PCSM	PCSM	*p*
No. patients (%)	382 (65.5)	201 (34.5)		494 (84.7)	89 (15.3)	
KLK3			< 0.001			< 0.001
Median (IQR)	3.8 (3.3–4.2)	3.5 (2.9–4.0)		3.8 (3.3–4.1)	3.1 (2.7–3.8)	
GGG no.(%%)			< 0.001			< 0.001
= < 2	211 (55.2)	38 (18.9)		237 (48.0)	12 (13.5)	
3	68 (17.8)	39 (19.4)		92 (18.6)	15 (16.9)	
4	42 (11.0)	30 (14.9)		60 (12.1)	12 (13.5)	
5	61 (16.0)	94 (46.8)		105 (21.3)	50 (56.2)	
pT Stage			< 0.001			< 0.001
pT2	181 (47.4)	50 (24.9)		208 (42.1)	23 (25.8)	
pT3a	135 (35.3)	61 (30.3)		171 (34.6)	25 (28.1)	
pT3b	66 (17.3)	90 (44.8)		115 (23.3)	41 (46.1)	
Preop. cPSA (ng/ml)			0.5			0.8
Median (IQR)	8.7 (5.8–13.5)	9.3 (6.1–15.0)		8.8 (5.8–13.8)	9.1 (6.1–15.0)	
LNI no. (%%)			< 0.001			< 0.001
No	346 (90.6)	143 (71.1)		427 (86.4)	62 (69.7)	
Yes	36 (9.4)	58 (28.9)		67 (13.6)	27 (30.3)	
BCR no.(%%)			< 0.001			< 0.001
No	235 (61.5)	1 (0.5)		236 (47.8)	0 (0.0)	
Yes	147 (38.5)	200 (99.5)		258 (52.2)	89 (100.0)	
Time to BCR (months)			< 0.001			< 0.001
Median (IQR)	72.0 (50.7–112.8)	13.3 (12.0–30.8)		60 (25.7–101.2)	12 (12.0–24.0)	
Metastasis no. (%%)	–	–	–			< 0.001
No	–	–	–	382 (77.3)	0 (0.0)	
Yes	–	–	–	112 (22.7)	89 (100.0)	
Time to MET (months)	–	–	–			< 0.001
Median (IQR)	–	–	–	84.0 (60.0–120.0)	36.0 (18.4–53.7)	
PCSM no.(%%)			< 0.001	–	–	–
No	382 (100.0)	112 (55.7)		–	–	–
Yes	0 (0.0)	89 (44.3)		–	–	–
Time to PCSM (months)			0.003	–	–	–
Median (IQR)	96.0 (69.5–131.6)	84.0 (56.3–123.5)		–	–	–

Metastases (MET) and Prostate Cancer Specific Mortality (PCSM) were coded as categorical variables with two levels (0 or 1). Data regarding time to the specific outcome were also obtained. **Abbreviations:** LNI (lymph node involvement at surgery); BCR (Biochemical recurrence); PCSM (Prostate cancer specific mortality). Statistical test: Kruskal-Wallis; significance level set: 0.05.

Table 5
UVA logistic regression analysis (Decipher®).

	BCR		Metastasis		PCSM	
	OR (95% CI)	*p*	*OR (95% CI)*	*p*	*OR (95% CI)*	*p*
KLK3	0.75 (0.6–0.91)	0.006	0.61 (0.49–0.74)	< 0.001	0.52 (0.41–0.66)	< 0.001
PSA_pre	1 (0.99–1.01)	0.958	1.01 (0.99–1.02)	0.296	1.01 (0.99–1.02)	0.44
pT stage						
pT3a	1.86 (1.27–2.75)	0.002	1.64 (1.06–2.53)	0.027	1.64 (0.72–2.43)	0.027
pT3b	4.08 (2.6–6.5)	< 0.001	4.94 (3.18–7.76)	< 0.001	4.94 (1.86–5.71)	< 0.001
GGG						
GGG3	1.3 (0.83–2.06)	0.257	1.3 (1.89–5.39)	0.257	1.3 (1.46–7.27)	0.257
GGG4	1.25 (0.74–2.13)	0.408	1.25 (2.21–7.12)	0.408	1.25 (1.68–9.32)	0.408
GGG5	2.81 (1.82–4.4)	< 0.001	2.81 (5.38–13.86)	< 0.001	2.81 (4.96–19.18)	< 0.001

Abbreviations: BCR (Biochemical recurrence); PCSM (Prostate cancer specific mortality).

presence of higher PSA levels.

As regard to the limits of this study, it must be mentioned that the use of PCa tissues rather than PCa-derived ECM did not allow us to associate the extent of PSA spillover in the tumor stroma to the extent of COL1A1 expression/cleavage. However, the grade and stage of our biobank specimens infer the brake of the basal membrane with the consequent leakage of PSA and tumor cell invasion. This is true also for the dataset samples. The second limit is due to the relatively small number of fresh PCa specimens (25 specimens) processed and analyzed in this study. This limit is, however, mitigated by the additional analysis of the 2 different, broad, datasets.

An inverse correlation between tPSA and clinical parameters has been recently reported [34,35]. By applying the Decipher® dataset, we also demonstrated that adding tPSA in the model eventually improved the ability to predict PCSM of Gleason-grade and pT. In both datasets and our human samples, tPSA did not parallel cPSA levels. In contrast, they were inversely associated. In particular, a more precise correspondence of tPSA over cPSA levels with the aggressiveness of the disease did emerge.

To understand the inverse correlations between tissue *KLK3*/PSA and tumor pathological features it is important to recall, first, that PSA is not a tumor specific marker but, rather, an organ specific marker (almost exclusively expressed by the prostate gland). Indeed, the increase of PSA in the blood does not necessarily indicate the presence of malignant prostate tumors. Second, it must be considered that PSA is a differentiation marker and PSA- tumors are, in their nature, more aggressive than PSA+ positive tumors [15,36]. This also explains, at least in part, the association of lower PSA levels to higher Gleason grade. Third, prostate cancer cells have been reported to express equal or even lower levels of PSA compared to normal prostate epithelial cells [15, 37–40]. In line with this, we also observed lower PSA expression in the tumor surgical resections compared to the non-tumor resections (**Suppl. Fig. 4**).

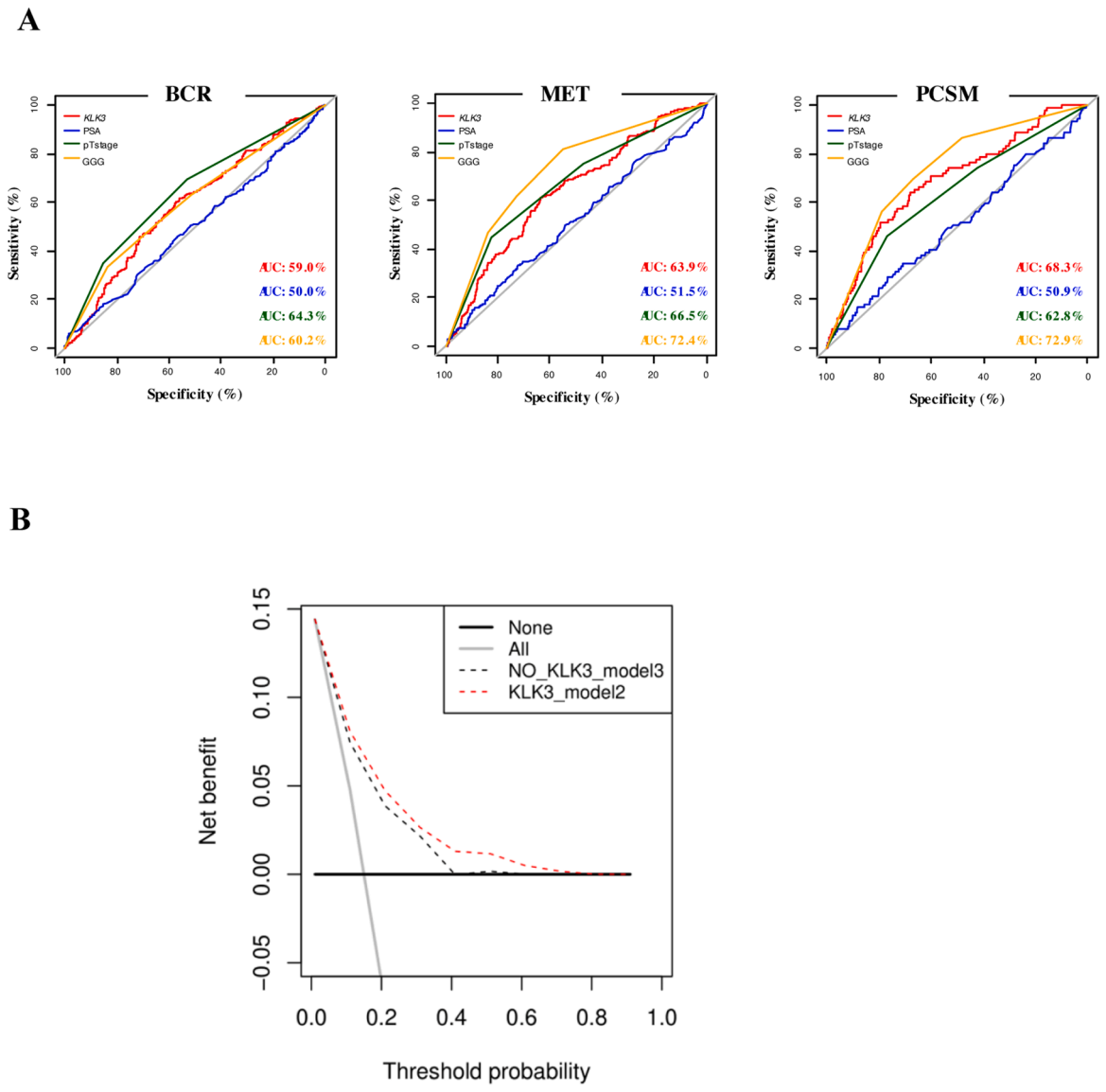

Fig. 3. ROC curves analysis (A) and Decision Curve Analysis (B) on Decipher® dataset. (A) ROC curves analysis demonstrating the discriminative ability of a univariable model for *KLK3* expression, preoperative PSA blood levels (PSA), pathological T stage (pT stage) and Gleason grade group (GGG) to predict biochemical recurrence (BCR), development of metastasis (MET) and PCa specific mortality (PCSM); (**B**) Decision curve analysis (DCA) demonstrating the net benefit associated with use of *KLK3* expression on MVA models to predict PCSM in comparison to MVA without *KLK3* expression.

Table 6
MVA model with *KLK3* (Decipher®).

	BCR OR (95% CI)	*p*-value	Metastasis OR (95% CI)	*p*-value	PCSM OR (95% CI)	*p*-value
KLK3	0.85 (0.69–1.06)	0.154	0.72 (0.57–0.91)	0.007	0.6 (0.46–0.78)	< 0.001
PSA	1 (0.99–1.02)	0.983	1.01 (1–1.03)	0.205	0.6 (0.46–0.78)	0.327
pT stage						
pT2	Ref (-)		Ref (-)		Ref (-)	
pT3a	1.79 (1.2–2.66)	0.004	1.53 (0.95–2.46)	0.079	0.6 (0.46–0.78)	0.619
pT3b	3.48 (2.19–5.6)	< 0.001	3.92 (2.42–6.41)	< 0.001	1.01 (0.99–1.02)	0.014
GGG						
GGG = < 2	Ref (-)		Ref (-)		Ref (-)	
GGG3	1.13 (0.71–1.82)	0.605	2.91 (1.69–5.06)	< 0.001	0.6 (0.46–0.78)	0.01
GGG4	1.18 (0.68–2.05)	0.561	3.88 (2.1–7.18)	< 0.001	1.01 (0.99–1.02)	0.005
GGG5	2.2 (1.39–3.5)	0.001	6.86 (4.22–11.36)	< 0.001	1.18 (0.62–2.24)	< 0.001

Abbreviations: BCR (Biochemical recurrence); PCSM (Prostate cancer specific mortality).

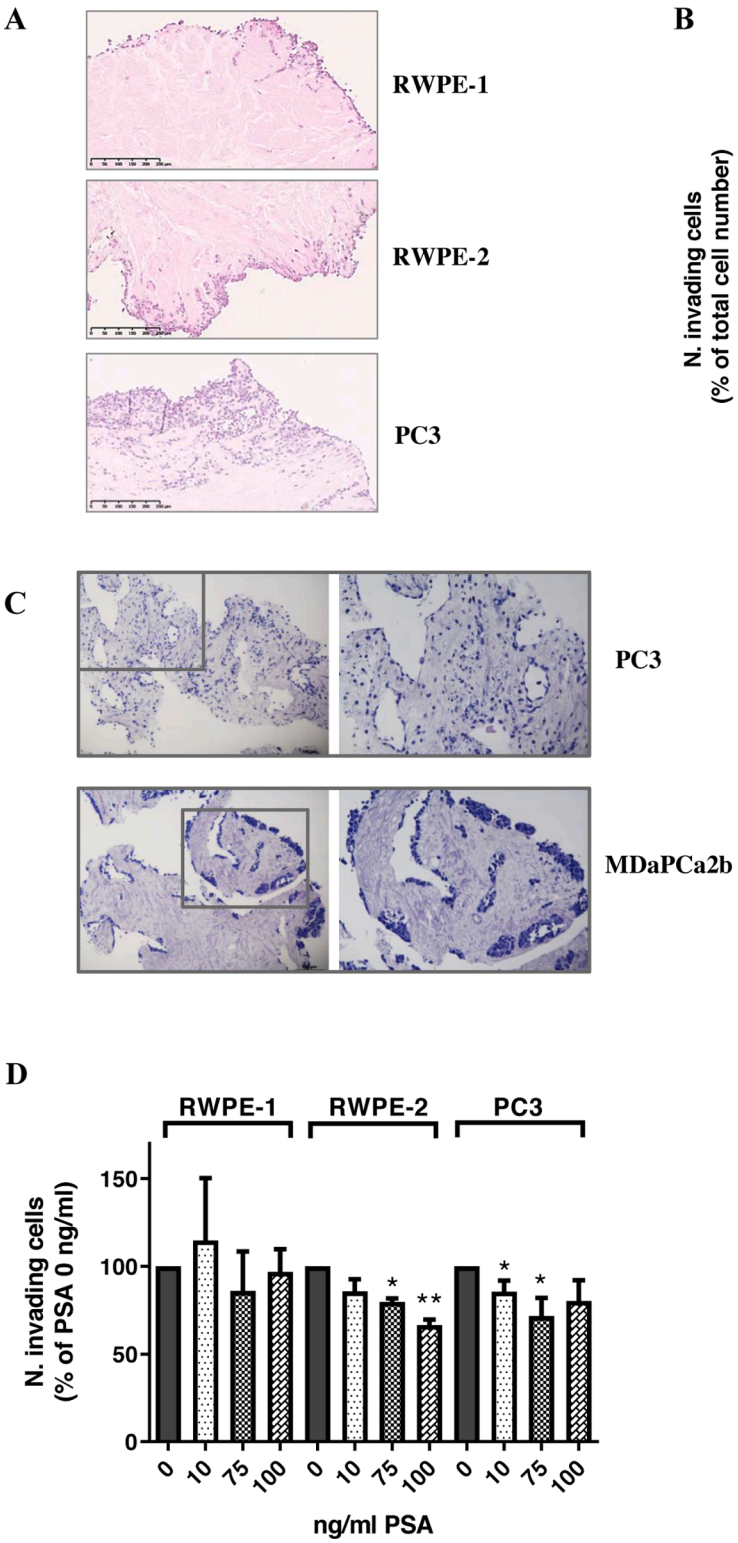

Fig. 4. Prostate-derived ECM invasion by PCa cells. Invasion of prostate tumor microenvironment by PCa cells was studied by using a 3D *ex-vivo/in-vitro* model consisting of prostate-derived extracellular matrix in co-culture with prostate cell lines. Cells were seeded on ECMs, placed into a 25 cm^2 sterile flask, at a density of 800,000/ml in the appropriate growth medium. After 1–3 days in the incubator, ECMs were transferred into a new flask with fresh medium which was replaced every 3–4 days for a total of 12 days. Thereafter, ECMs from co-cultures were fixed in 10% buffered formalin for 24–48 h at room temperature, embedded in paraffin and processed for haematoxylin and eosin (H&E) staining. ECM local invasion by prostate cell lines was quantified by counting the number of infiltrated cells on at least 3 FOVs (Fields of View)/slice of ECM. At least 3 slices/ECM were considered for cell quantification. In order to avoid misinterpretations due to either a different cell doubling-time or the different size of the ECM slices, the number of invading cells was normalized to the number of total cells (*i.e.*, invading + non-invading cells). (**A**) Representatives FOVs of H&E-stained non tumoral-prostate derived ECM, co-cultured with RWPE-1, RWPE-2 or PC3 cell lines. Cells within the ECM are considered as invading cells, whereas the cells along the outer border and along the lumen as well as cells located in the cavities of the ECM are considered as non-invading. (**B**) Quantification of invading cells from ECM-cells co-cultures. Plot showing number of invading cells, expressed as a percentage of the total number of cells; (**C**) Representatives 10-fold-magnified FOVs (left panels) and 20-fold-magnified FOVs (right panels) of H&E-stained non tumoral-prostate derived ECM, co-cultured with the PSA- PC3 cells or the PSA+ MDaPCa2b cells. A totally different pattern of invasion is evident as the PC3 completely and uniformly invaded the matrix, whereas the MDaPCa2b were not able to infiltrate the matrix but got stuck on the outer border and along the lumen of the matrix; (**D**) Plot showing the effect of PSA treatment on invasion ability of prostate cells. For each cell line the number of invading cells, normalized to the number of total cells, is expressed as a percentage of untreated cells. At least 3 FOVs/slice/sample have been counted. * $p < 0.05$; ** $p < 0.01$. Mann-Whitney *U* test.

Finally, our findings demonstrating an anti-metastatic role of PSA, also help to understand the inverse correlation between tPSA and tumor progression.

The reliability of our findings is supported by Stege and colleagues, who were able to demonstrate the superiority of bioptic tPSA (rather than the cPSA) in predicting the outcome of endocrine treatment in metastatic PCa patients [41]. In addition, Bonk and colleagues recently assessed the prognostic/diagnostic utility of PSA-immunostaining by analyzing large tissue microarrays; they found a link between reduced PSA staining intensity with unfavorable tumor phenotype and poor prognosis [35]. However, it must be noticed that both methods as well as the outcome of our study are not of immediate clinical translation as they are based on subjective, semiquantitative assessments of PSA thresholds. Future studies should aim to establish reproducible cut-offs, which must be defined according to specific clinical/pathological parameters [42]. Regardless of the feasibility to immediately translate

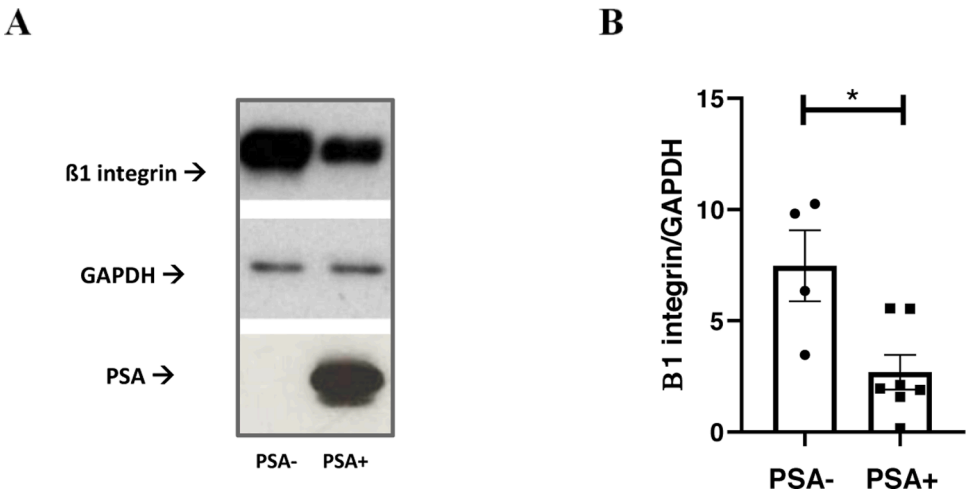

Fig. 5. Beta 1 integrin expression in PCa specimens. Beta 1 integrin, PSA and GAPDH levels were assessed by western blot analyze in surgical resections from RP. Specimens are from our institutional biobank. Equal micrograms of tissue lysate were loaded. (**A**) Representative blot images showing Beta 1 integrin, PSA and GAPDH expression; **(B)** Plot showing quantification of Beta 1 integrin, normalized to the levels of GAPDH according to PSA levels. *$p < 0.05$; Mann-Whitney test.

tPSA quantification to the clinical practice, current findings are of major relevance since they clarified at least one of the mechanisms underneath the correlation between higher tPSA levels and a lower tumor malignancy, with all its clinical implications. Moreover, having recognized a protective role of tPSA over the steps of PCa invasion may also have important speculative implications in terms of future choice or refinement of neoadjuvant treatments.

Conclusions

Together with previous evidences [34,37], our data demonstrate that tPSA content and its activity in the tumor microenvironment are inversely correlated to cPSA and to tumor progression. Likewise, we provide novel evidence that tPSA can cleave also COL1A1, one of the most abundant ECM proteins, and interfere with the integrin-mediated matrisome signaling, thus being potentially able to control cells path through the ECM and their migration ability. Moreover, we demonstrated that tPSA levels improve PCSM prediction, which is of high clinical relevance for its consequences in terms of tailored treatment choices. Therefore, a deeper knowledge of PSA role throughout PCa pathobiology is relevant to make the most of this biomarker in terms of disease prognosis.

CRediT authorship contribution statement

Francesco Pellegrino: Formal analysis, Investigation, Methodology, Validation, Writing – original draft, Writing – review & editing. **Arianna Coghi:** Investigation, Visualization. **Giovanni Lavorgna:** Formal analysis, Investigation, Methodology, Validation, Visualization. **Walter Cazzaniga:** Formal analysis, Investigation, Methodology, Visualization. **Edoardo Guazzoni:** Investigation, Methodology. **Irene Locatelli:** Investigation, Project administration, Validation, Visualization. **Isabella Villa:** Investigation, Methodology. **Simona Bolamperti:** Investigation, Validation. **Nadia Finocchio:** Visualization. **Massimo Alfano:** Methodology. **Roberta Lucianò:** Investigation, Methodology. **Alberto Briganti:** Validation. **Francesco Montorsi:** Resources. **Andrea Salonia:** Conceptualization, Resources, Project administration, Resources, Writing – review & editing. **Ilaria Cavarretta:** Conceptualization, Formal analysis, Investigation, Methodology, Project administration, Supervision, Validation, Visualization, Writing – original draft, Writing – review & editing.

Declaration of Competing Interest

The authors declare no conflict of interest.

Funding

This research did not receive any specific grant from funding agencies in the public, commercial, or not-for-profit sectors.

Acknowledgments

The authors thank R. Jeffrey Karnes (Mayo Clinic), Eric A. Klein (Cleveland Clinic), Robert B. Den (Thomas Jefferson University), Stephen J. Freedland (Cedars Sinai), Edward M. Schaeffer (Johns Hopkins/Northwest University) and Decipher Biosciences for access to tumor pathology, outcomes & transcriptomic data.

Supplementary materials

Supplementary material associated with this article can be found, in the online version, at doi:10.1016/j.tranon.2021.101211.

References

[1] R.L. Siegel, K.D. Miller, A. Jemal, Cancer statistics 2018, CA Cancer J. Clin. 68 (2018) 7–30.
[2] https://uroweb.org/guideline/prostate-cancer 2021.
[3] H. Lilja, D. Ulmert, A.J. Vickers, Prostate-specific antigen and prostate cancer: prediction, detection and monitoring, Nat. Rev. Cancer 8 (2008) 268–278.
[4] A.R. Rao, H.G. Motiwala, O.M. Karim, The discovery of prostate-specific antigen, BJU Int. 101 (2008) 5–10.
[5] B.A. Mahal, A.A. Aizer, J.A. Efstathiou, P.L. Nguyen, Association of very low prostate-specific antigen levels with increased cancer-specific death in men with high-grade prostate cancer, Cancer 122 (2016) 78–83.
[6] B.B. McGuire, B.T. Helfand, S. Loeb, Q. Hu, D. O'Brien, P. Cooper, et al., Outcomes in patients with Gleason score 8-10 prostate cancer: relation to preoperative PSA level, BJU Int. 109 (2012) 1764–1769.
[7] K.C. Koo, S.U. Park, K.H. Kim, K.H. Rha, S.J. Hong, S.C. Yang, et al., Predictors of survival in prostate cancer patients with bone metastasis and extremely high prostate-specific antigen levels, Prostate Int. 3 (2015) 10–15.
[8] S.A. Williams, P. Singh, J.T. Isaacs, S.R. Denmeade, Does PSA play a role as a promoting agent during the initiation and/or progression of prostate cancer? Prostate 67 (2007) 312–329.
[9] E.P. Diamandis, Prostate-specific antigen: a cancer fighter and a valuable messenger? Clin. Chem. 46 (2000) 896–900.
[10] A.H. Fortier, B.J. Nelson, D.K. Grella, J.W. Holaday, Antiangiogenic activity of prostate-specific antigen, J. Natl. Cancer Inst. 91 (1999) 1635–1640.
[11] A.P. Cumming, S.N. Hopmans, S. Vukmirovic-Popovic, W.C. Duivenvoorden, PSA affects prostate cancer cell invasion *in vitro* and induces an osteoblastic phenotype in bone *in vivo*, Prostate Cancer Prostatic Dis. 14 (2011) 286–294.

[12] S. Altuwaijri, Role of prostate specific antigen (PSA) in pathogenesis of prostate cancer, J. Cancer Ther. 3 (2012) 331–336.
[13] A. Moradi, S. Srinivasan, J. Clements, J. Batra, Beyond the biomarker role: prostate-specific antigen (PSA) in the prostate cancer microenvironment, Cancer Metastasis Rev. 38 (2019) 333–346.
[14] K.W. Watt, P.J. Lee, T. M'Timkulu, W.P. Chan, R. Loor, Human prostate-specific antigen: structural and functional similarity with serine proteases, PNAS 83 (1986) 3166–3170.
[15] J.A. Schalken, Molecular and cellular prostate biology: origin of prostate-specific antigen expression and implications for benign prostatic hyperplasia, BJU Int. 93 (Suppl 1) (2004) 5–9.
[16] S.R. Denmeade, L.J. Sokoll, D.W. Chan, S.R. Khan, J.T. Isaacs, Concentration of enzymatically active prostate-specific antigen (PSA) in the extracellular fluid of primary human prostate cancers and human prostate cancer xenograft models, Prostate 48 (2001) 1–6.
[17] M.M. Webber, A. Waghray, D. Bello, Prostate-specific antigen, a serine protease, facilitates human prostate cancer cell invasion, Clin. Cancer Res. 1 (1995) 1089–1094.
[18] J.M. Mattsson, S. Ravela, C. Hekim, M. Jonsson, J. Malm, A. Närvänen, et al., Proteolytic activity of prostate specific antigen (PSA) towards protein substrates and effect of peptides stimulating PSA activity, PLoS ONE 19 (2014), e107819.
[19] Cancer Genome Atlas Research Network, The molecular taxonomy of primary prostate cancer, Cell 163 (2015) 1011–1025.
[20] D.E. Spratt, M. Alshalalfa, N. Fishbane, A.B. Weiner, R. Mehra, B.A. Mahal, et al., Transcriptomic heterogeneity of androgen receptor activity defines a *de novo* low ar-active subclass in treatment naïve primary prostate cancer, Clin. Cancer Res. 25 (2019) 6721–6730.
[21] W. Cazzaniga, M. Nebuloni, E. Longhi, I. Locatelli, R. Allevi, R. Lucianò, et al., Human prostate tissue-derived extracellular matrix as a model of prostate microenvironment, Eur. Urol. Focus 2 (2016) 400–408.
[22] K. Malinowska, H. Neuwirt, I.T. Cavarretta, J. Bektic, H. Steiner, H. Dietrich, et al., Interleukin-6 stimulation of growth of prostate cancer in vitro and in vivo through activation of the androgen receptor, Endocr. Relat. Cancer 16 (2009) 155–169.
[23] M. Nebuloni, L. Albarello, A. Andolfo, C. Magagnotti, L. Genovese, I. Locatelli, et al., Insight on colorectal carcinoma infiltration by studying perilesional extracellular, Matrix Sci. Rep. 6 (2016) 22522.
[24] L. Genovese, L. Zawada, A. Tosoni, A. Ferri, P. Zerbi, R. Allevi, et al., Cellular localization, invasion, and turnover are differently influenced by healthy and tumor-derived extracellular matrix, Tissue Eng. Part A 20 (2014) 2005–2018.
[25] D. Cunningham, Z. You, *In vitro* and in vivo model systems used in prostate cancer research, J. Biol. Methods 2 (2015) e17.
[26] E.C. Brockbank, J. Bridges, C.J. Marshall, E. Sahai, Integrin beta1 is required for the invasive behaviour but not proliferation of squamous cell carcinoma cells *in vivo*, Br. J. Cancer 92 (2005) 102–112.
[27] M. Li, J. Wang, C. Wang, L. Xia, J. Xu, X. Xie, et al., Microenvironment remodeled by tumor and stromal cells elevates fibroblast-derived COL1A1 and facilitates ovarian cancer metastasis, Exp. Cell Res. 394 (2020), 112153.
[28] C.L. Hall, C.W. Dubyk, T.A. Riesenberger, D. Shein, E.T. Keller, K.L. van Golen, Type I collagen receptor (alpha2beta1) signaling promotes prostate cancer invasion through RhoC GTPase, Neoplasia 10 (2008) 797–803.
[29] A. Fenner, Prostate cancer: PSA enzymatic activity to assess disease aggressiveness, Nat. Rev. Urol. 10 (2013) 557.
[30] M.J. Ahrens, P.A. Bertin, E.F. Vonesh, T.J. Meade, W.J. Catalona, D. Georganopoulou, PSA enzymatic activity: a new biomarker for assessing prostate cancer aggressiveness, Prostate 73 (2013) 1731–1737.
[31] S. Vukmirovic-Popovic, N.G. Escott, W.G.M. Duivenvoorden, Presence and enzymatic activity of prostate-specific antigen in archival prostate cancer samples, Oncol. Rep. 20 (2008) 897–903.
[32] C.J. Wolfe, I.S. Kohane, A.J. Butte, Systematic survey reveals general applicability of "guilt-by-association" within gene coexpression networks, BMC Bioinform. 6 (2005) 227.
[33] A.H. Fortier, B.J. Nelson, D.K. Grella, Holaday, Antiangiogenic activity of prostate-specific antigen, J. Natl. Cancer Inst. 91 (1999) 1635–1640.
[34] X. Liu, X. Chen, K. Rycaj, H.P. Chao, Q. Deng, C. Jeter, et al., Systematic dissection of phenotypic, functional, and tumorigenic heterogeneity of human prostate cancer cells, Oncotarget 15 (2015) 23959–23986.
[35] S. Bonk, M. Kluth, C. Hube-Magg, A. Polonski, G. Soekeland, G. Makropidi-Fraune, et al., Prognostic and diagnostic role of PSA immunohistochemistry: a tissue microarray study on 21,000 normal and cancerous tissues, Oncotarget 10 (2019) 5439–5453.
[36] B.A. Mahal, D.D. Yang, N.Q. Wang, M. Alshalalfa, E. Davicioni, V. Choeurng, et al., Clinical and genomic characterization of low-prostate-specific antigen, high-grade prostate cancer, Eur. Urol. 74 (2018) 146–154.
[37] A. Magklara, A. Scorilas, C. Stephan, G.O. Kristiansen, S. Hauptmann, K. Jung, et al., Decreased concentrations of prostate-specific antigen and human glandular kallikrein 2 in malignant versus nonmalignant prostatic tissue, Urology 1 (2000) 527–532.
[38] S.D. Qiu, C.Y. Young, D.L. Bilhartz, J.L. Prescott, G.M. Farrow, W.W. He, et al., *In situ* hybridization of prostate-specific antigen mRNA in human prostate, J. Urol. 144 (1990) 1550–1556.
[39] T.G. Pretlow, T.P. Pretlow, B. Yang, C.S. Kaetzel, C.M. Delmoro, S.M. Kamis, et al., Tissue concentrations of prostate-specific antigen in prostatic carcinoma and benign prostatic hyperplasia, BB Int. J. Cancer 49 (1991) 645–649.
[40] L. Hakalahti, P. Vihko, P. Henttu, H. Autio-Harmainen, Y. Soini, R. Vihko, Evaluation of PAP and PSA gene expression in prostatic hyperplasia and prostatic carcinoma using northern-blot analyze, *in situ* hybridization and immunohistochemical stainings with monoclonal and bispecific antibodies, Int. J. Cancer 49 (1991) 645–649.
[41] R. Stege, M. Grande, K. Carlström, B. Tribukait, A. Pousette, Prognostic significance of tissue prostate-specific antigen in endocrine-treated prostate carcinomas, Clin. Cancer Res. 6 (2000) 160–165.
[42] S. Draghici, P. Khatri, A.C. Eklund, Z. Szallasi, Reliability and reproducibility issues in DNA microarray measurements, Trends Genet. 22 (2006) 101–109.